This is the accepted manuscript (postprint) of the following article:
Oskouei, H. I., Aghamohammadi, H., & Eslami-Farsani, R. (2022). Electrochemical performance of TiNb2O7 nanoparticles anchored with different contents of MWCNTs as anode materials for Li-ion batteries. *Ceramics International*, *48*(10), 14717-14725.
https://doi.org/10.1016/j.ceramint.2022.02.007

Electrochemical performance of $TiNb_2O_7$ nanoparticles anchored with different contents of MWCNTs as anode materials for Li-ion batteries

Hesam Iranipour Oskouei, Hamed Aghamohammadi [*], Reza Eslami-Farsani [*]

Faculty of Materials Science and Engineering, K. N. Toosi University of Technology, Tehran, Iran

[*] *Corresponding authors: eslami@kntu.ac.ir, hamed.aghamohammadi@outlook.com*

Abstract

In this study, the electrochemical behavior of titanium niobium oxide (TNO) composites with 1, 3, and 5 wt.% of multi-walled carbon nanotubes (MWCNTs) was investigated. The results showed a significant improvement in the electrochemical performance of TNO by the addition of MWCNTs in terms of initial capacity, rate performance, and rate capability. The initial capacity of pure TNO at 0.1C increased from 251.6 mAh/g to 272.4, 302.2, and 265.9 mAh/g by addition of 1, 3, and 5 wt.% of MWCNTs, respectively. Furthermore, the cyclic stability of the samples improved considerably by the addition of the MWCNTs; the capacity value of pure TNO after 200 cycling at 1C was only 78.3 mAh/g while for TNO/3 wt.% MWCNTs was about 145.6 mAh/g. Similarly, the rate performance of the TNO/MWCNTs nanocomposites was better than pure TNO in all charge/discharge rates. The MWCNTs contents in nanocomposites had significant effects on their performance in which the optimal content of MWCNTs in this study was 3 wt.%. The results showed that the presence of MWCNTs in nanocomposites created a conductive network with good ionic and electrical conductivity and thus, improved the rate performance of samples. In addition, the stresses caused by the intercalation/deintercalation of Li-ions were moderated by MWCNTs, improving the cyclic stability.

Keywords: Li-ion batteries, Titanium niobium oxide, CNTs, Nanocomposites, Electrochemical performance

1- Introduction

In this age of technology, electrochemical energy storage devices such as batteries and supercapacitors have found great applications. As the most essential type of rechargeable batteries, Li-ion batteries (LIBs), owing to their outstanding properties such as high energy density and high working voltage, are used in various vehicles such as electric cars, smartphones,

This is the accepted manuscript (postprint) of the following article:
Oskouei, H. I., Aghamohammadi, H., & Eslami-Farsani, R. (2022). Electrochemical performance of TiNb2O7 nanoparticles anchored with different contents of MWCNTs as anode materials for Li-ion batteries. *Ceramics International*, *48*(10), 14717-14725.
https://doi.org/10.1016/j.ceramint.2022.02.007

and laptops. However, several challenges such as capacity fading after cycling, especially at high charge/discharge rates, can be introduced as the strong barrier to using LIBs in applications with the mentioned requirements. The electrochemical performance of LIBs is dependent mainly on the characteristics of their electrodes and many researchers have focused on improving their performances in terms of cyclic stability, rate performance, and safety [1-11].

According to the literature, the used anode materials for LIBs can be classified into three different categories of intercalation-deintercalation anodes (such as hard carbon and graphite) [12-15], alloying-dealloying anodes (such as silicon, germanium, and tin) [16-19], and conversion anodes (such as Fe_2O_3) [20-22]. The Li-ion storage mechanism of the conversion anode materials, which include oxides, nitrides, and phosphides, is based on the occurrence of a conversion reaction in which an intermediate element is oxidized. Also, the alloying reaction between Li-ions and metal in alloying anode materials results in high specific capacity values of 660-4200 mAh/g. Although both conversion and alloying anode materials have high specific capacity values, their poor cyclic stability because of high volume changes during the charge/discharge process has restricted their wide application in LIBs [23].

Intercalation/ deintercalation anodes can be divided into two main groups of carbon-based materials (such as graphite, graphene, and hard carbon), and titanium-based materials. In literature, the specific capacities of 200-1100 mAh/g and 170-380 mAh/g respectively have been reported for carbon-based materials group and titanium-based materials. Although the capacity values of these types of anodes are lower than those of conversation and alloying anodes, their outstanding properties such as high safety, good cyclability, and high working potential, made them promising anodes for practical application in LIBs. Graphite, due to its attractive properties such as high accessibility, thermally/ chemically/ mechanically stability, and extremely low cost, is the most common type of carbon-based anodes in LIBs. Despite its attractive features, it still suffers from some issues such as irreversible reaction with the electrolyte and cathodic decomposition of electrolyte results in the formation of solid electrolyte interphase (SEI) layer on its surface. The formation of the SEI layer has adverse effects on safety, cyclic stability, rate capability and generally limits the performance of the LIBs. Therefore, developing new anode materials with high safety for the next generation of LIBs is necessary [23].

Similar to graphite and graphene as layered materials, recently a new class of two-dimensional materials named MXenes has been introduced for LIBs anodes. MXenes can be

This is the accepted manuscript (postprint) of the following article:
Oskouei, H. I., Aghamohammadi, H., & Eslami-Farsani, R. (2022). Electrochemical performance of TiNb2O7 nanoparticles anchored with different contents of MWCNTs as anode materials for Li-ion batteries. *Ceramics International*, *48*(10), 14717-14725.
https://doi.org/10.1016/j.ceramint.2022.02.007

obtained by the selective etching of the MAX phases. Recently, many researchers have focused on the Li-ion storage capability of the MXenes and MXene-based composites. Although the Li-ion storage capability of the MXenes can be improved significantly by various methods such as altering their functional groups, they have limited Li-ion storage capability. On the other hand, MXene-based composites are good candidates as anode materials for LIBs. Restricting the occurrence of restacking phenomenon for the MXenes and also buffering the volumetric expansion and loss of electrical contact of high-capacity anode materials are two aims of preparation of the MXene-based composites [7, 24-28].

As another type of Intercalation/ deintercalation anodes, Ti-based anode materials, because of their high working voltage, have been introduced as safe anodes for LIBs. These groups of anodes, with their proper safety, good cyclic stability, and limited formation of SEI layer, have presented good electrochemical properties. Lithium titanium oxides (LTO) are the most widely known Ti-based anode materials. LTO with the specific capacity of 175 mAh/g at the constant potential of 1.55 V can place a maximum of 3 Li-ions in its structure with a volume expansion of just 0.2%, which makes it a zero-strain anode compound. Long cyclic stability and low cost make LTO an interesting choice for LIBs. However, the low specific capacity and low electrical/ ionic conductivity of LTO restricted their application for fast-charge LIBs [29-31].

As a newly-introduced type of Ti-based anode material, titanium niobium oxide (TNO) compounds with a general formula $TiNb_xO_{2+2.5x}$ have been introduced as an alternative for LTO. According to the x value in the general formula of $TiNb_xO_{2+2.5x}$, the theoretical capacity of TNO compounds can be calculated as follows [29]:

$$C = 403 - 5441/(133x + 80)\ (mAh/g) \quad (1)$$

Up to now, $TiNb_2O_7$ (x=2) [32], $Ti_2Nb_{10}O_{29}$ (x=5) [33], $TiNb_6O_{17}$ (x=6) [34], and $TiNb_{24}O_{62}$ (x=24) [35] with respectively theoretical capacity values of 387, 396, 396, and 401 mAh/g have been reported as the main compounds of TNO family materials for electrochemical energy storage. Like LTO, the TNO anode materials have high safety and high cyclic stability. Although the capacity value of the TNO is higher than LTO, their electrical/ ionic conductivity is poor, restricting their rate performance [9, 36, 37]. Up to now, different approaches, including synthesis of TNO nanostructures, morphological controlling, formation of porous TNO, the introduction of dopant in TNO structure, and formation of TNO composites with conductive materials, have been proposed for solving the low-rate capability of TNO [38-43].

This is the accepted manuscript (postprint) of the following article:
Oskouei, H. I., Aghamohammadi, H., & Eslami-Farsani, R. (2022). Electrochemical performance of TiNb2O7 nanoparticles anchored with different contents of MWCNTs as anode materials for Li-ion batteries. *Ceramics International*, *48*(10), 14717-14725.
https://doi.org/10.1016/j.ceramint.2022.02.007

Up to now, different conductive materials such as graphene and carbon coatings have been used for improving the rate performance of TNO anodes, especially $TiNb_2O_7$ and $Ti_2Nb_{10}O_{29}$. However, there are very limited studies on the influence of carbon nanotubes (CNTs) on the performance of TNO. CNTs, due to their high electrical conductivity, are the proper choices for improving the rate performance of the Ti-based anodes. For example, Lin et al. [44] synthesized $TiNb_2O_7$ /CNTs nanocomposites and studied their electrochemical performance. Their findings showed that $TiNb_2O_7$ /CNTs nanocomposites had superior electrochemical performance. For example, $TiNb_2O_7$ /CNTs nanocomposites delivered a specific capacity value of 163 mAh/g at 30C. Also, the samples presented outstanding cyclic stability in which high-capacity retention of 97.6% after 100 cycles at 10C was achieved. In another work, Liu et al. [45] also compared the electrochemical performance of $TiNb_2O_7$ and $TiNb_2O_7$ /CNTs-ketjen black (KB) anodes prepared by spray-drying and solvothermal methods. $TiNb_2O_7$ /CNTs-KB showed both excellent rate capability and cyclic performance. For example, after 1000 cycles at 5C, the specific capacity of $TiNb_2O_7$ /CNTs-KB nanocomposites decreased from 220 to 145.4 mAh/g (33.9% reduction), while the capacity values of pure $TiNb_2O_7$ reduced from 180 to 80 mAh/g (55% reduction).

In a recent study, Zhu et al. [46] optimized the electrochemical performance of $TiNb_2O_7$ /C/CNTs microspheres. $TiNb_2O_7$ /C and $TiNb_2O_7$ /C/CNTs samples were prepared by ball milling followed by the spray-drying method. The result was $TiNb_2O_7$/ultrathin carbon layer and, also a structure of $TiNb_2O_7$ /C entangled into CNTs network and a highly conductive porous $TiNb_2O_7$ /C/CNTs microsphere. Electrochemical investigation showed exceptional cyclic durability with charge capacities of 343.3 mAh/g at 0.25 C after 300 cycles and 274.9 mAh/g at 10 C after 1000 cycles.

To the best of the author's knowledge, the performed works have used only a constant content of CNTs for the synthesis of their samples, and there is no experimental investigation on the effects of CNTs on the performance of $TiNb_2O_7$ anode materials. Thereby, this work aims to synthesize the $TiNb_2O_7$ anodes with different weight percentages of multi-walled CNTs (MWCNTs) and investigate their electrochemical performance as anode materials for LIBs.

2- Experimental procedure

2-1- Synthesis of $TiNb_2O_7$

This is the accepted manuscript (postprint) of the following article:
Oskouei, H. I., Aghamohammadi, H., & Eslami-Farsani, R. (2022). Electrochemical performance of TiNb2O7 nanoparticles anchored with different contents of MWCNTs as anode materials for Li-ion batteries. *Ceramics International*, *48*(10), 14717-14725.
https://doi.org/10.1016/j.ceramint.2022.02.007

In this study, $TiNb_2O_7$/CNTs were synthesized by combining solvothermal and ultrasonication methods. At first, for the synthesis of $TiNb_2O_7$ nanoparticles, the stoichiometric amounts of $NbCl_5$ (Sigma Aldrich) and tetrabutyl titanate (Sigma Aldrich) were used as Nb and Ti precursors were added to 70 ml absolute ethanol (99.99% Merck) and the mixture was stirred for 20 min at room temperature. After that, 3 wt.% of HNO_3-treated MWCNTs were added to the mixture. Then, the mixed solution was transferred to a 100 ml Teflon-lined stainless-steel autoclave. After that, the solvothermal treatment was done at 200 ºC for 24 h and then, the collected powders were filtered and washed with deionized water several times. The obtained product was calcinated at 900 °C for 5 h under the air atmosphere. The calcination process under the air atmosphere through the burning of the MWCNTs and the formation of CO_2 gas restrict the growth of the $TiNb_2O_7$ nanoparticles.

After synthesizing $TiNb_2O_7$ nanoparticles, the obtained $TiNb_2O_7$ powders were added to deionized water, and then, different contents of the MWCNTs (1, 3, and 5 wt.%) were added to the mixture. Then, the mixtures were sonicated for 15 min, and then, the filtration and drying steps were conducted to obtain the $TiNb_2O_7$/MWCNTs nanocomposites. The samples with 1, 3, and 5 wt.% MWCNTs respectively are named as TNO/1wt.% MWCNTs, TNO/3wt.% MWCNTs and TNO/5wt.% MWCNTs.

2-2- Structural and morphological characterization

The crystal structure of as-prepared samples was determined by X-ray diffraction (XRD, Rigaku Ultima IV) with Cu Kα radiation (λ=1.5406 Å) in 2θ range of 5 to 80 and with a step of 0.02 degree. The Raman analysis was conducted by Teksan takram-N1-541 Raman Microscope with 532 nm laser in 100 to 4600 RS range. To investigate the structure and morphology of the samples, the field emission scanning electron microscope (FESEM, TESCAN MIRA3TESCAN-XMU) was used.

2-3- Electrochemical characterizations

To investigate the electrochemical behavior of samples, CR2032 half cells were assembled. The positive electrodes (cathode) were prepared by the coating of a slurry composed of 80 wt.% active materials (nanocomposites), 10 wt.% polyvinylidene fluoride (PVDF) as a binder, and 10 wt.% conductive super-P as a conductive agent on copper foils, followed by drying in a vacuum

This is the accepted manuscript (postprint) of the following article:
Oskouei, H. I., Aghamohammadi, H., & Eslami-Farsani, R. (2022). Electrochemical performance of TiNb2O7 nanoparticles anchored with different contents of MWCNTs as anode materials for Li-ion batteries. *Ceramics International*, *48*(10), 14717-14725.
https://doi.org/10.1016/j.ceramint.2022.02.007

at 105 °C for 10 h. After that, the 2032-type of half-cells were assembled using Li-foil as the anode, lithium hexafluorophosphate ($LiPF_6$, 1M) as the electrolyte, and polypropylene membrane as a separator. The electrochemical measurements in the voltage range of 1 to 3 V (vs. Li^+/Li) at 25 ºC were done using a battery testing instrument (NEWARE 4000, China). To further investigate the electrochemical properties of samples, the electrochemical impedance spectroscopies (EIS) were carried out at the frequency range of 100 to 0.01 Hz using a potentiostat instrument (RADSTAT 10, Kianshardanesh, Iran).

3- Results and discussion

3-1- Structural analyses

The structural studies of TNO/MWCNTs nanocomposites are done using XRD and Raman analyses. The XRD patterns of the TNO, TNO nanocomposites with 1, 3, and 5 wt.% MWCNTs are shown in Fig. 1. As can be seen, all diffraction patterns are similar and the main peaks have appeared at the same positions and no evidence of peak shifting can be seen in XRD patterns. For all samples, all the diffraction peaks match with the reference pattern of $TiNb_2O_7$, and no impurities can be found. Also, it is worth noting that the diffraction peaks related to CNTs cannot be seen individually in the respective patterns due to their overlap with $TiNb_2O_7$ diffraction peaks.

This is the accepted manuscript (postprint) of the following article:
Oskouei, H. I., Aghamohammadi, H., & Eslami-Farsani, R. (2022). Electrochemical performance of TiNb2O7 nanoparticles anchored with different contents of MWCNTs as anode materials for Li-ion batteries. *Ceramics International*, *48*(10), 14717-14725.
https://doi.org/10.1016/j.ceramint.2022.02.007

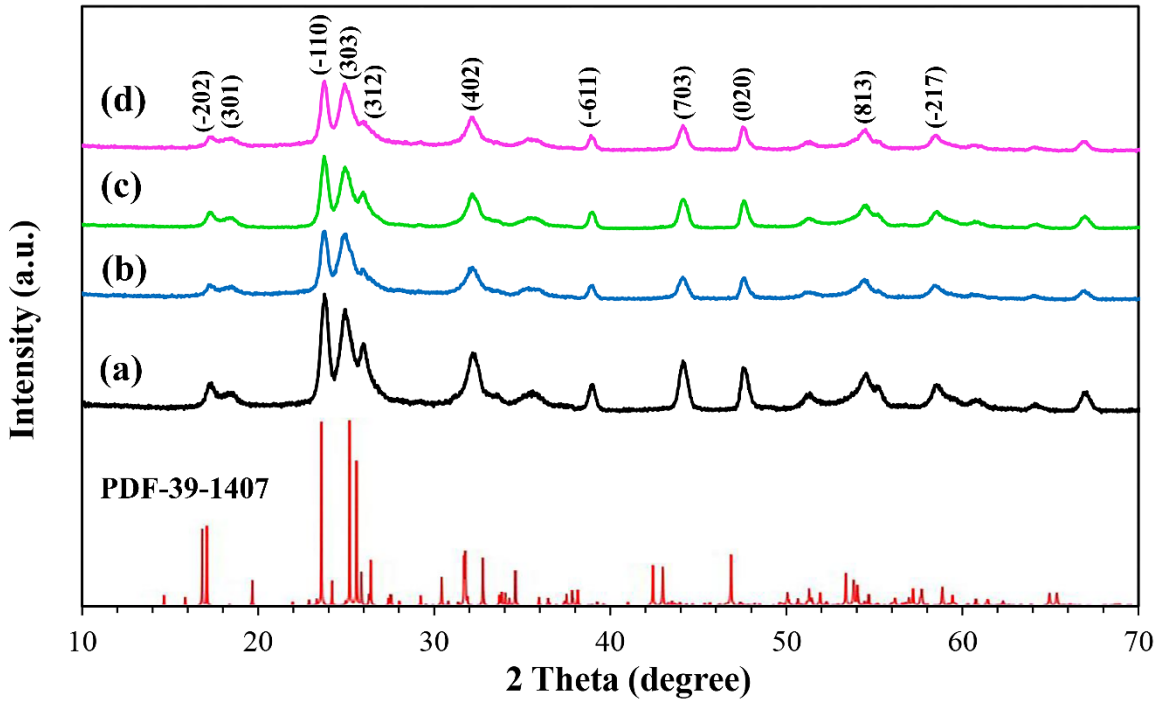

Fig. 1. XRD patterns of (a) TNO, (b) TNO/1 wt.% MWCNTs, (c) TNO/3 wt.% MWCNTs and (d) TNO/5 wt.% MWCNTs nanocomposites.

The pure TNO and TNO/MWCNTs nanocomposites were also investigated by Raman analysis, as shown in Fig. 2. As can be seen, the TNO sample consisted of peaks related to TNO bonds located at 238, 668, 993 cm^{-1}, respectively associated with the O-Ti-O and O-Nb-O bonds, edge-shared TiO_6, and corner-shared NbO_6 octahedra [47, 48]. Moreover, in addition to the related peaks of TiNb2O7, the D and G peaks can be found in the Raman spectra of the TNO/MWCNTs nanocomposites, demonstrating the presence of MWCNTs in their stricture.

This is the accepted manuscript (postprint) of the following article:
Oskouei, H. I., Aghamohammadi, H., & Eslami-Farsani, R. (2022). Electrochemical performance of TiNb2O7 nanoparticles anchored with different contents of MWCNTs as anode materials for Li-ion batteries. *Ceramics International*, *48*(10), 14717-14725.
https://doi.org/10.1016/j.ceramint.2022.02.007

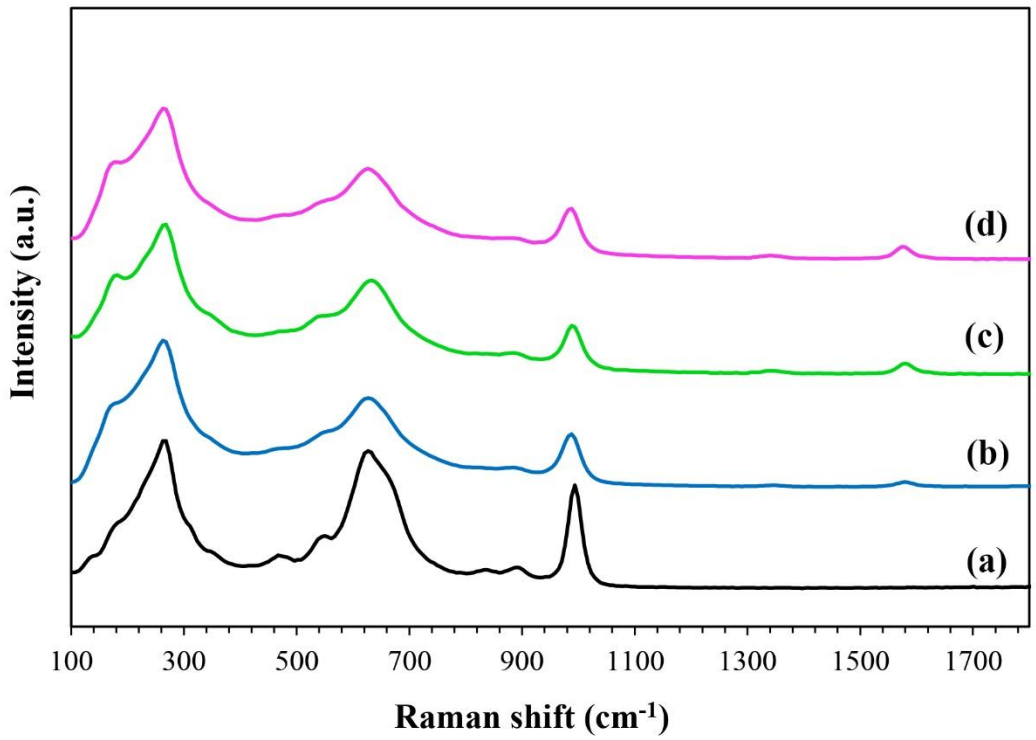

Fig. 2. Raman spectra of (a) TNO, (b) TNO/1 wt.% MWCNTs, (c) TNO/3 wt.% MWCNTs and (d) TNO/5 wt.% MWCNTs nanocomposites.

Fig. 3 presents the FESEM images of the TNO sample. As can be seen, the $TiNb_2O_7$ nanoparticles with a size range of 50 nm to 70 nm have been formed by mentioned approaches. Moreover, the energy dispersive spectroscopy (EDS)-mapping analysis also demonstrates the successful synthesis of pure $TiNb_2O_7$. The formation of well-distributed nanoparticles without agglomeration can be related to the presence of MWCNTs and the formation of CO_2 during calcination in the air atmosphere, inhibiting the occurrence of growth phenomenon. The FESEM images of the TNO/MWCNTs nanocomposites are given in Fig. 4. As can be seen in the FESEM image, the TNO/1 wt.% MWCNTs nanocomposite (Fig. 4a), there is no sign of MWCNTs agglomeration, but their amount for constructing the continuous network is not enough. However, by increasing the content of MWCNTs to 3 wt.% (Fig. 4b), the uniform distribution and dispersion of the MWCNTs can be seen. On the other hand, it can be seen in Fig. 4c that further increasing the MWCNTs content in samples resulted in severe agglomeration and their inferior dispersion/distribution.

This is the accepted manuscript (postprint) of the following article:
Oskouei, H. I., Aghamohammadi, H., & Eslami-Farsani, R. (2022). Electrochemical performance of TiNb2O7 nanoparticles anchored with different contents of MWCNTs as anode materials for Li-ion batteries. *Ceramics International*, *48*(10), 14717-14725.
https://doi.org/10.1016/j.ceramint.2022.02.007

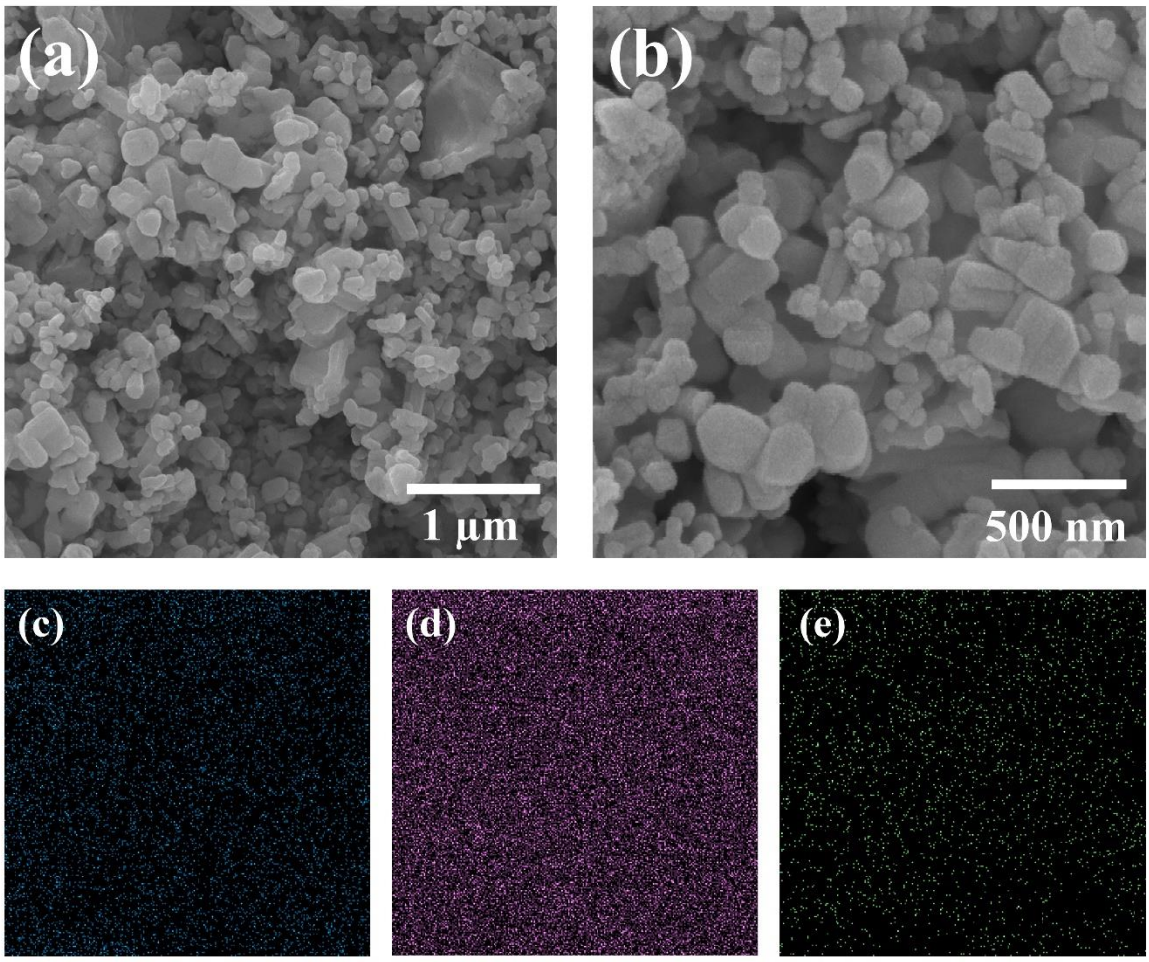

Fig. 3. Morphological characterization of TNO sample, (a and b) The FESEM images of TNO samples at different magnifications along with EDS-mapping of the (c) Ti, (d) Nb, and (e) O elements.

This is the accepted manuscript (postprint) of the following article:
Oskouei, H. I., Aghamohammadi, H., & Eslami-Farsani, R. (2022). Electrochemical performance of TiNb2O7 nanoparticles anchored with different contents of MWCNTs as anode materials for Li-ion batteries. *Ceramics International*, *48*(10), 14717-14725.
https://doi.org/10.1016/j.ceramint.2022.02.007

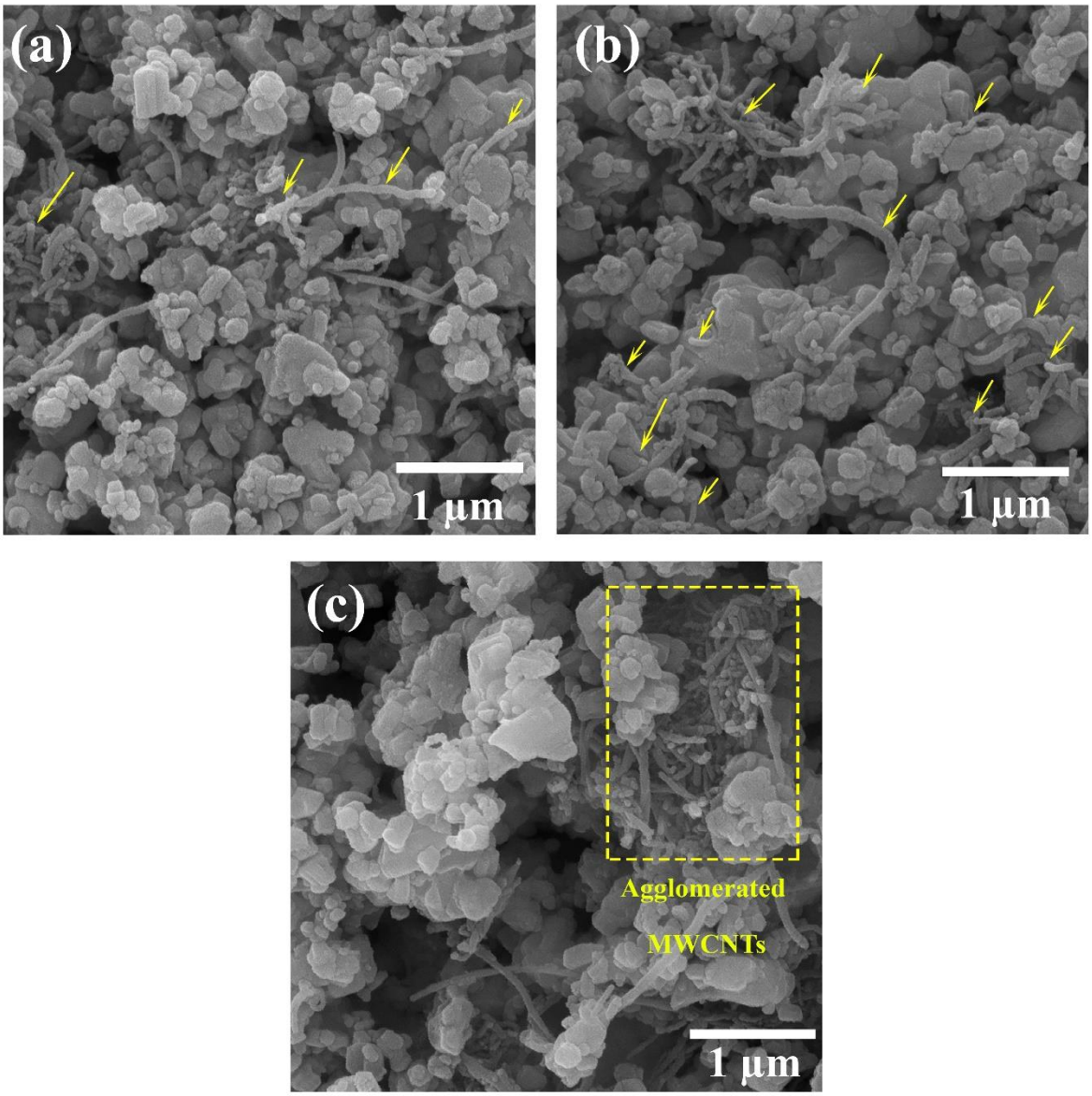

Fig. 4. FESEM images of (a) TNO/1 wt.% MWCNTs, (b) TNO/3 wt.% MWCNTs and (c) TNO/5 wt.% MWCNTs nanocomposites.

3-2- Electrochemical performance

As mentioned in the experimental section, the electrochemical characterizations of the LIBs half-cell configuration were investigated in a voltage range of 1.0 to 3.0 V (vs. Li/Li^+). The first charge-discharge curves of TNO/MWCNTs nanocomposites at 0.1C (1C= 387 mAh/g) are shown in Fig. 5. As can be seen, for all samples, the charge-discharge profile can be divided into three regions. The plateau region at about 1.65 V is related to typical phase changing and solid solution

This is the accepted manuscript (postprint) of the following article:
Oskouei, H. I., Aghamohammadi, H., & Eslami-Farsani, R. (2022). Electrochemical performance of TiNb2O7 nanoparticles anchored with different contents of MWCNTs as anode materials for Li-ion batteries. *Ceramics International*, *48*(10), 14717-14725.
https://doi.org/10.1016/j.ceramint.2022.02.007

mechanism and it also indicates the redox reaction of Ti^{3+}/Ti^{4+}, Nb^{4+}/Nb^{5+}. As can be seen, the pure TNO sample presented an initial discharge capacity of 251.6 mAh/g. On the other hand, the initial discharge capacity values for the TNO/1 wt.% MWCNTs, TNO/3 wt.% MWCNTs, and TNO/5 wt.% MWCNTs nanocomposites were respectively 272.4, 302.2, and 265.90 mAh/g. These values are respectively about 8.26%, 20.11%, and 5.68% higher than that of the pure TNO sample. These results show that the effectiveness of MWCNTs in improving the electrochemical performance of TNO is related to its content.

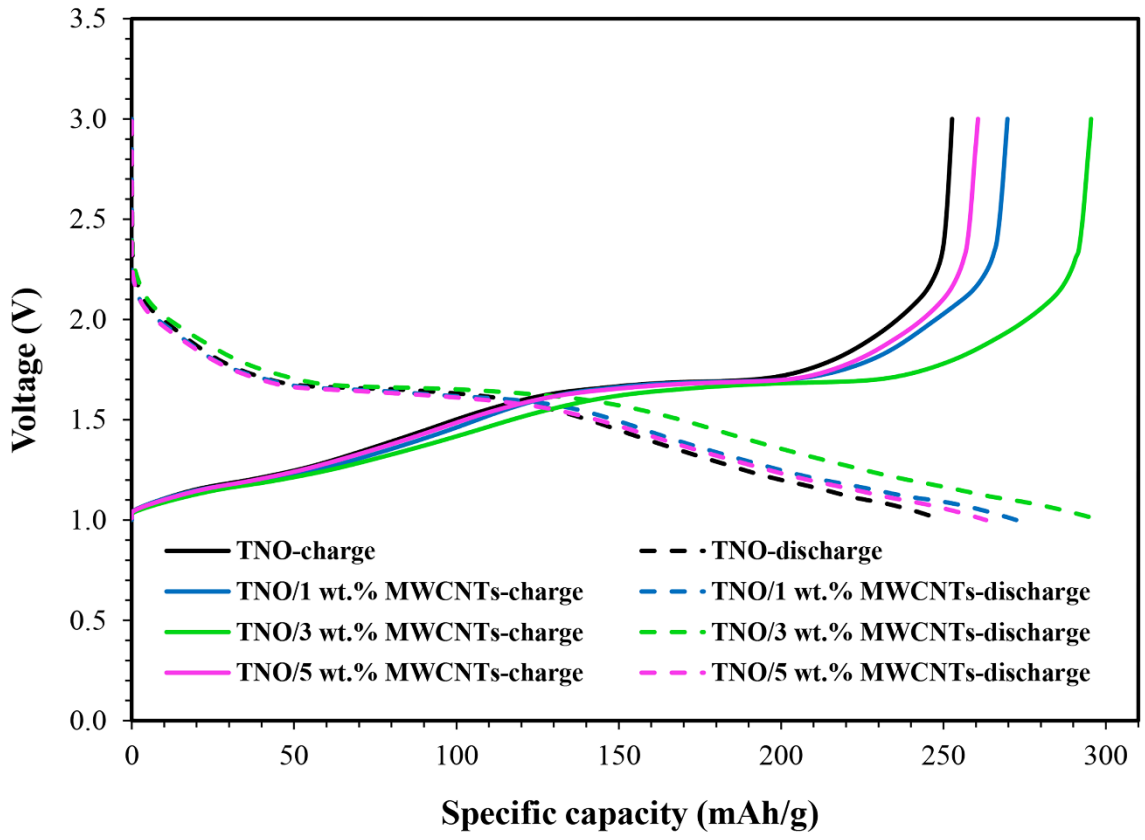

Fig. 5. First charge/discharge profiles of TNO and TNO/MWCNTs nanocomposites at C/10 (1C =387 mA/g).

To identify the rate capability of samples, the electrochemical tests were performed at different charge/discharge rates from C/5 to 20C. The charge/discharge curves at different rates, the rate capability, and polarization values of samples as a function of C-rates are shown in Fig. 6. As can be seen, by increasing the charge/discharge rates from C/5 to 2C, the capacity fading of

the TNO/MWCNTs nanocomposites is lower than that of pure TNO samples, especially samples with higher contents of MWCNTs. For example, concerning the discharge capacity values at C/5, the capacity of TNO, TNO/1 wt.% MWCNTs, TNO/3 wt.% MWCNTs, and TNO/5 wt.% MWCNTs decreased by 33.53%, 34%, 23.5%, and 24.46% by increasing the charge/discharge rates to 2C. Moreover, it is evident that up to 2C, the discharge capacity of TNO/3 wt.% MWCNTs is higher than those of other samples while at higher rates of 5C and 10C, the TNO/5 wt.% MWCNTs presented better electrochemical performance. For example, at a high rate of 5C, the average discharge capacity values of 113.03, 119.58, 115.85, and 154.4 mAh/g were respectively achieved for TNO/1 wt.% MWCNTs, TNO/3 wt.% MWCNTs, and TNO/5 wt.% MWCNTs nanocomposites. Furthermore, the charge/discharge rate decreased from 20C to C/5 to determine capacity retention. It is obvious that all samples showed great capacity retention; the capacity retention values for pure TNO, TNO/1 wt.% MWCNTs, TNO/3 wt.% MWCNTs, and TNO/5 wt.% MWCNTs samples were 94.09, 91.15, 94.13, and 93.60 %, respectively.

By more accurate investigation of charge-discharge profiles (Figs. 6a to 6d), it can be found that by increasing the current rates from C/5 to 20C, the difference between the charge plateau and discharge plateau potentials of samples increased, significantly. This means that the redox reactions occurred at a higher potential for higher current rates. The higher polarization results in higher capacity fading of samples. The polarization of the pure TNO and TNO/MWCNTs nanocomposites in different rates from C/5 to 5C is shown in Fig. 6e. The polarization values were calculated by measuring the difference between the charge and discharge profiles. As can be seen, there is a negligible difference between the polarization of pure and nanocomposites at low C-rates. However, by increasing the C-rate, the polarization of pure TNO increased significantly, which is remarkably higher than that of TNO/MWCNTs nanocomposites. The higher capacity fading of the pure TNO sample at high rates can be related to its higher polarization. Interestingly, the lowest polarization values have been obtained for TNO/3 wt.% MWCNTs nanocomposites which this observation is in good agreement with its lower capacity fading. Regarding the polarization results and the lower amount of it for the TNO/MWCNTs composite samples, it can be concluded that the presence of MWCNTs with their exceptional ionic and electrical conductivity. These features caused faster transportation of Li^+ ions and electrons and therefore, the electrochemical performance kinetics have been improved.

From the presented results, it can be deduced that the TNO/3 wt.% MWCNTs and TNO/5 wt.% MWCNTs have better electrochemical performances over other samples. It seems that the content of MWCNTs in TNO/1 wt.% MWCNTs is not enough for creating a conductive network, as shown in FESEM images. Moreover, the appropriate content and good dispersion of the MWCNTs in TNO/3 wt.% MWCNTs is the main reason for its improved performance. On the other hand, although by increasing the contents of MWCNTs to 5 wt.%, the charge transfer is facilitated, their inferior dispersing can inhibit the Li-ion diffusion (Fig. 4c). These results are in good agreement with the results of Lee et al. [49]. They investigated the effects of different contents of CNTs (1, 3, and 5 wt.%) on the electrochemical performance of LTO as supercapacitors. The rate capability of the pure LTO and LTO/CNTs nanocomposites was investigated at different ranges from 0.5 A/g to 6 A/g. Their results showed that compared with pure LTO, the LTO/1 wt.% CNTs, LTO/ 3 wt.% CNTs had higher capacity values at all charge/discharge rates. However, their results indicated that the addition of 5 wt.% MWCNTs had negative effects on the electrochemical performance of LTO. The EIS analyses of their work showed that the lowest charge transfer resistance and polarization were achieved for the LTO/ 3 wt.% CNTs. However, excessive contents of MWCNTs above 3 wt.% resulted in the occurrence of agglomeration phenomenon and consequently, increased the polarization.

This is the accepted manuscript (postprint) of the following article:
Oskouei, H. I., Aghamohammadi, H., & Eslami-Farsani, R. (2022). Electrochemical performance of TiNb2O7 nanoparticles anchored with different contents of MWCNTs as anode materials for Li-ion batteries. *Ceramics International*, *48*(10), 14717-14725.
https://doi.org/10.1016/j.ceramint.2022.02.007

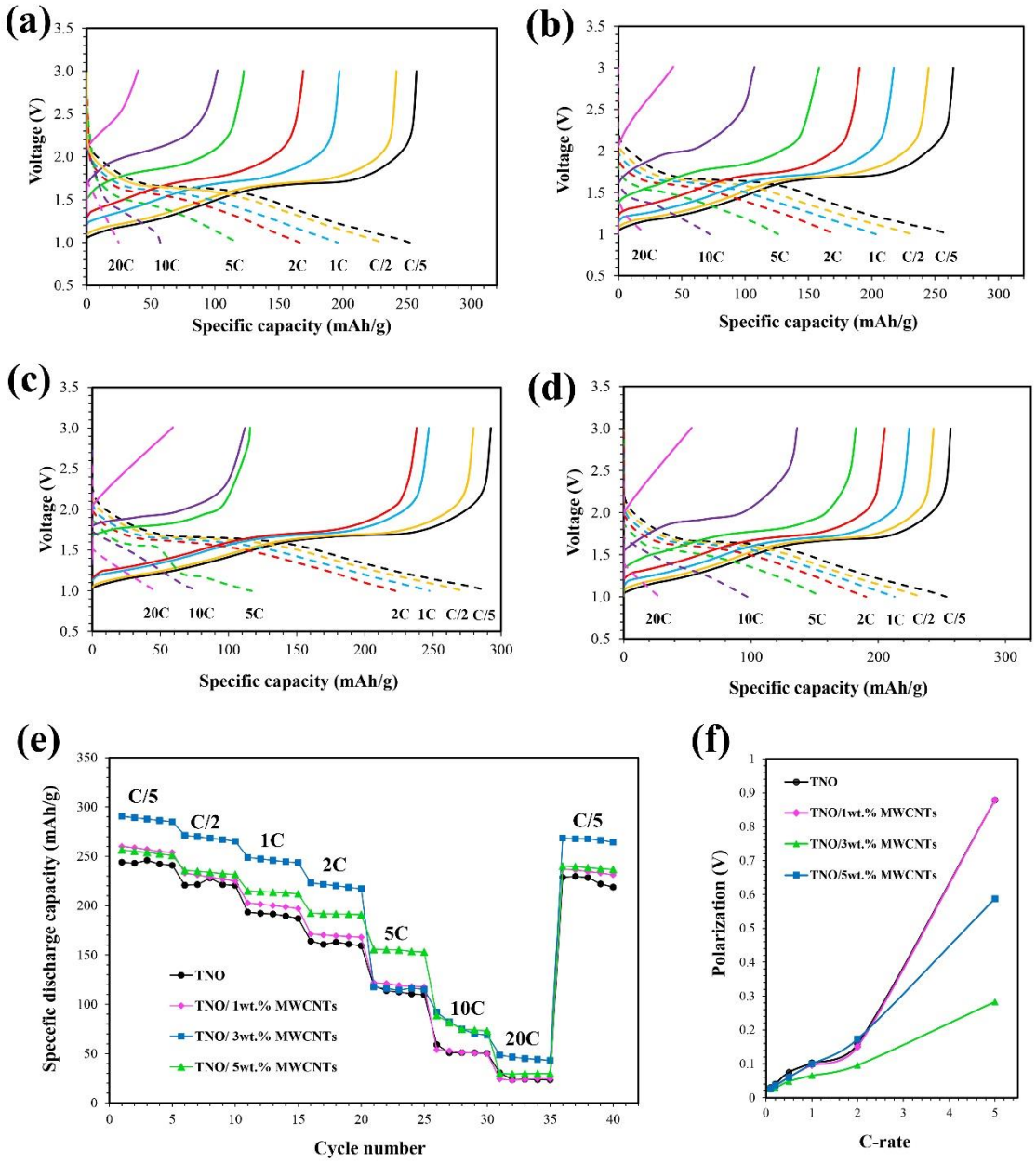

Fig. 6. Electrochemical performance of TNO and TNO/MWCNTs nanocomposites at different rates from C/5 to 20C; charge-discharge profiles at different rates of (a) TNO, (b) TNO/1 wt.% MWCNTs, (c) TNO/3 wt.% MWCNTs, (d) TNO/5 wt.% MWCNTs, (e) rate capability of samples, and (f) polarization values of the sample as a function of C-rate.

To identify the reasons for the improved rate performance of TNO/MWCNTs nanocomposites over the TNO sample, the EIS analysis was conducted, as shown in Fig. 7. It is worth noting that the EIS analyses were conducted after rate capability tests at discharge state.

This is the accepted manuscript (postprint) of the following article:
Oskouei, H. I., Aghamohammadi, H., & Eslami-Farsani, R. (2022). Electrochemical performance of TiNb2O7 nanoparticles anchored with different contents of MWCNTs as anode materials for Li-ion batteries. *Ceramics International*, *48*(10), 14717-14725.
https://doi.org/10.1016/j.ceramint.2022.02.007

Fig. 7a shows the Nyquist plots of TNO and TNO/MWCNTs samples which all curves consist of two depressed semicircles and a straight line and the fitted equivalent circuit is shown in inst of Fig. 7a. The first semicircle that appeared at high-frequency regions relates to the SEI layer resistance (R_{SEI}). The second semicircle at the high-frequency area is representative of charge transfer resistance (R_{ct}). The linear area that is called the Warburg line became evident at the low-frequency region.

The calculated R_{SEI} and R_{ct} values of all samples are presented in Table 1. As can be seen, R_{SEI} values of TNO decreased by adding all contents of MWCNTs in the TNO/MWCNTs nanocomposites. However, the Rct values were only reduced by adding the 3 and 5 wt.% MWCNTs. In other words, a decreasing tendency is for Rct is observed as a function of MWCNTs. The low content of MWCNTs in TNO/1 wt.% MWCNTs can be introduced as the main reason to describe why its Rct value is not as low as other TNO/MWCNTs samples. On the other hand, the Rct values TNO/3 wt.% MWCNTs and TNO/5 wt.% MWCNTs samples are about 50% lower than the TNO sample.

Table 1. Calculated values of the impedance and Li-ion diffusion coefficient of samples

Sample	Rs (Ω)	R_{SEI} (Ω)	R_{ct} (Ω)	D_{Li+} (cm^2/s)
TNO	2.543	8.436	10.41	3.02×10^{-11}
TNO/1 wt.% MWCNTs	2.19	6.565	10.27	3.89×10^{-11}
TNO/3 wt.% MWCNTs	2.758	6.377	5.762	7.50×10^{-11}
TNO/5 wt.% MWCNTs	2.968	6.508	5.371	5.34×10^{-11}

This is the accepted manuscript (postprint) of the following article:
Oskouei, H. I., Aghamohammadi, H., & Eslami-Farsani, R. (2022). Electrochemical performance of TiNb2O7 nanoparticles anchored with different contents of MWCNTs as anode materials for Li-ion batteries. *Ceramics International*, *48*(10), 14717-14725.
https://doi.org/10.1016/j.ceramint.2022.02.007

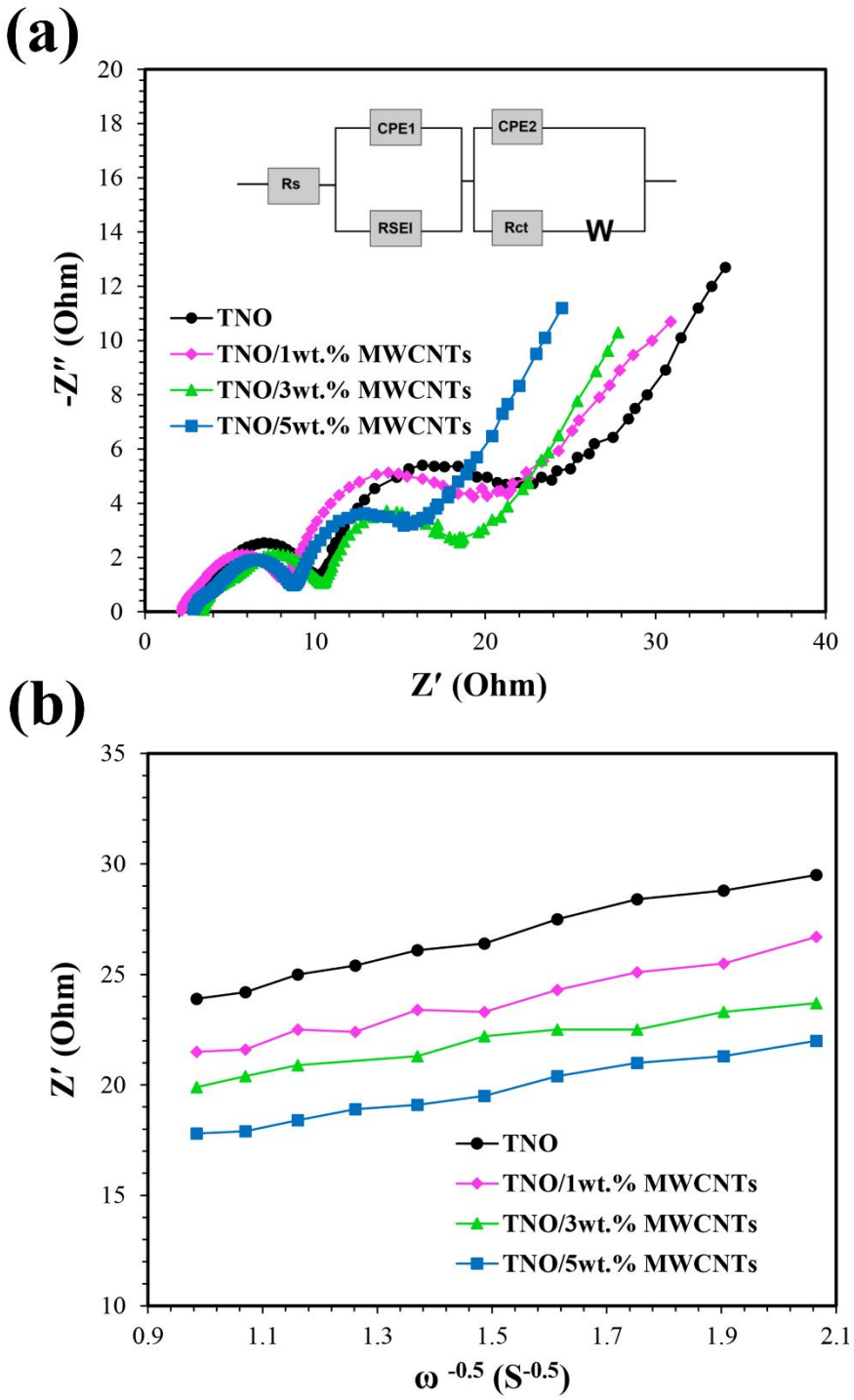

Fig. 7. EIS results of TNO and TNO/MWCNTs samples; (a) Nyquist plots and (b) $Z' - \omega^{-0.5}$ plots at low-frequency region.

In addition to the charge transfer and electrical conductivity of anode materials, the Li-ion diffusion is another critical factor in their electrochemical performance. The Li-ion diffusion

This is the accepted manuscript (postprint) of the following article:
Oskouei, H. I., Aghamohammadi, H., & Eslami-Farsani, R. (2022). Electrochemical performance of TiNb2O7 nanoparticles anchored with different contents of MWCNTs as anode materials for Li-ion batteries. *Ceramics International*, *48*(10), 14717-14725.
https://doi.org/10.1016/j.ceramint.2022.02.007

coefficient (D_{Li+}) can be calculated using the Z'-$\omega^{0.5}$ plot at low-frequency region according to the following equations [50]:

$$D_{Li} = \frac{R^2T^2}{2A^2n^2F^4C^2\sigma^2} \quad (1)$$

$$Z' = R_1 + R_{SEI} + R_{ct} + \sigma\omega^{(-1/2)} \quad (2)$$

Where T is the absolute temperature (298.15 K), R is the gas constant (8.314 J), n is the number of electrons per molecule during oxidizing, A is the surface area of the electrode (1.53 cm^2). Also, F is the Faradays' constant (96485.33 Cal/mol), C is the molar concentration of Li-ion (4.17×10^{-3} $mol.cm^{-3}$), ω is the angular frequency and σ is Warburg factor ($\Omega/S^{1/2}$) [50, 51]. The σ is the slope of Z' - $\omega^{-0.5}$ plots at the low-frequency region. The D_{Li+} values have been calculated and presented in Table 1. As can be seen, the D_{Li+} values of all TNO/MWCNTs are higher than that of TNO samples. The D_{Li+} values of 3.02×10^{-11}, 3.89×10^{-11}, 7.50×10^{-11}, and 5.34×10^{-11} cm^2/s have been achieved for TNO, TNO/1 wt.% MWCNTs, TNO/3 wt.% MWCNTs, and TNO/5 wt.% MWCNTs, respectively. The lower D_{Li+} of TNO/5 wt.% MWCNTs compared with TNO/3 wt.% MWCNTs can be related to the high probability of agglomeration phenomenon.

Another essential requirement of LIBs is their cyclic stability. Fig. 8 shows the charge/discharge curves and cyclic stability of the samples at 1C. The first specific discharge capacity for the TNO sample at 1C rate is 221.4 mAh/g while its value decreased to 78.3 mAh/g after 200 cycles (65% reduction). However, it can be seen that by the presence of MWCNTs not only the first discharge capacity value of the samples has been increased, but also cyclic stability of samples improved. In other words, the initial specific discharge capacity for TNO/1 wt.% MWCNTs, TNO/3 wt.% MWCNTs, and TNO/5 wt.% MWCNTs was 233.5, 257.6, and 229.5 mAh/g, which respectively decreased to 91.12, 145.6, and 108.8 mAh/g after 200 cycles. In other words, the capacity retention of TNO, TNO/1 wt.% MWCNTs, TNO/3 wt.% MWCNTs, and TNO/5 wt.% MWCNTs after 200 cycles are about 35%, 39%, 56.5%, and 47.7%, respectively.

This is the accepted manuscript (postprint) of the following article:
Oskouei, H. I., Aghamohammadi, H., & Eslami-Farsani, R. (2022). Electrochemical performance of TiNb2O7 nanoparticles anchored with different contents of MWCNTs as anode materials for Li-ion batteries. *Ceramics International*, *48*(10), 14717-14725.
https://doi.org/10.1016/j.ceramint.2022.02.007

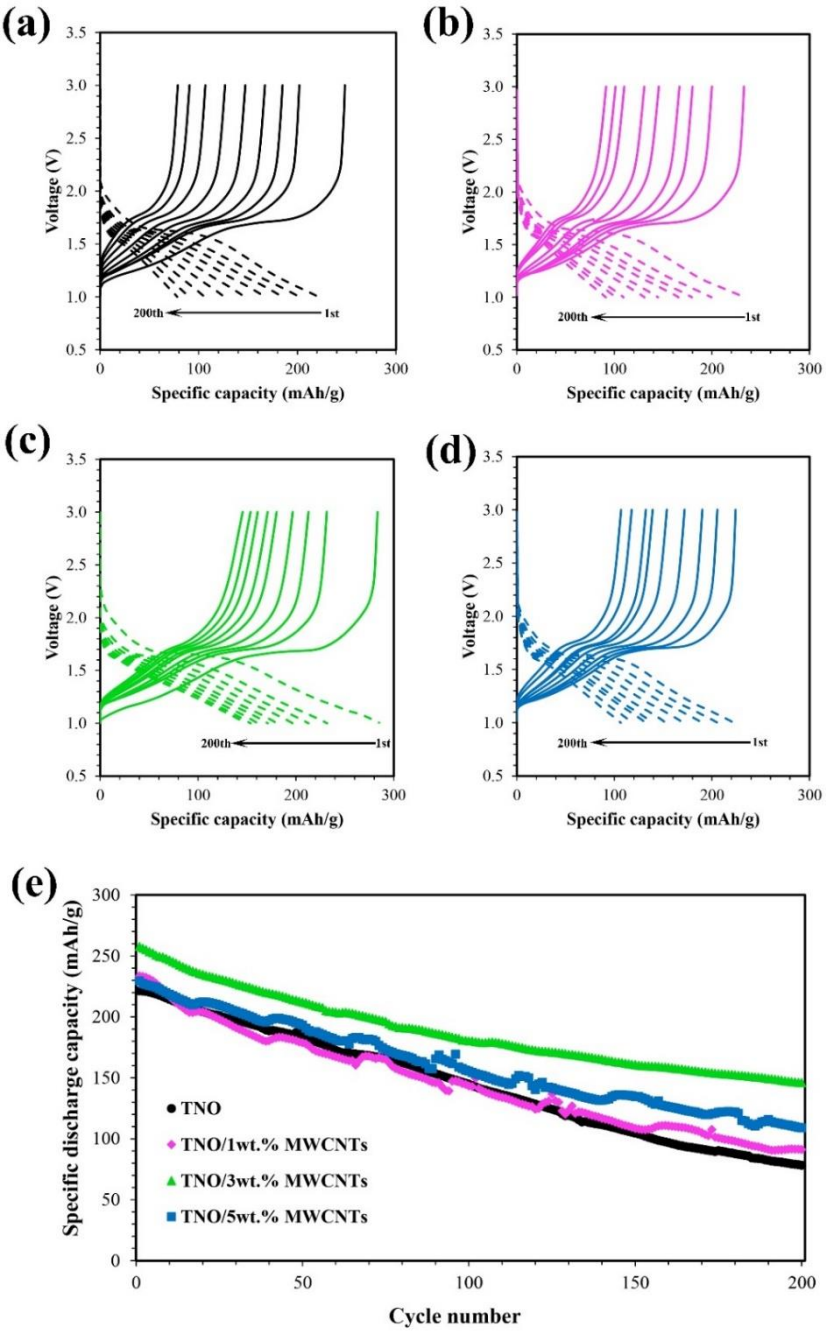

Fig. 8. Cyclic stability of TNO and TNO/MWCNTs samples at 1C; charge-discharge profiles at different cycle numbers of (a) TNO, (b) TNO/1 wt.% MWCNTs, (c) TNO/3 wt.% MWCNTs, (d) TNO/5 wt.% MWCNTs, (e) comparison of cyclic stability of samples.

To further investigate the reasons for the better cyclic performance of TNO/MWCNTs composites compared with pure TNO sample, the surface morphology of TNO and TNO/5 wt.% MWCNTs were evaluated using FESEM images, as shown in Fig. 9. As shown in Fig. 9a, there

This is the accepted manuscript (postprint) of the following article:
Oskouei, H. I., Aghamohammadi, H., & Eslami-Farsani, R. (2022). Electrochemical performance of TiNb2O7 nanoparticles anchored with different contents of MWCNTs as anode materials for Li-ion batteries. *Ceramics International*, *48*(10), 14717-14725.
https://doi.org/10.1016/j.ceramint.2022.02.007

are many microcracks for TNO samples that these cracks could be caused by volume changes of the TNO during charge/discharge processes. However, no visible cracks can be found for the TNO/5 wt.% MWCNTs, which can be attributed to the presence of MWCNTs in their structure. Therefore, the high capacity fading of the pure TNO can be attributed to these cracks. According to these observations, it can be said that the MWCNTs act as a stress relaxing agent and so, improve the cyclic stability of samples. Accordingly, the higher cyclic stability of the TNO/3 wt.% MWCNTs compared with all samples can be related to the proper dispersion and distribution of MWCNTs.

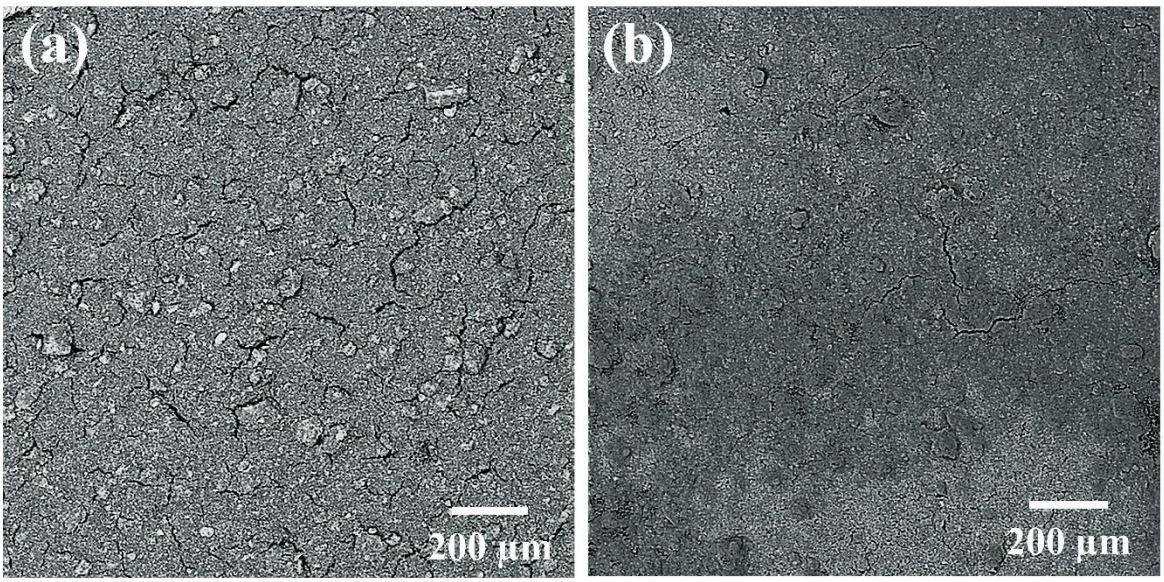

Fig. 9. The FESEM image of electrode film after 200 cycles for (a) TNO and (b) TNO/5 wt.% MWCNTs.

4- Conclusion

In this research, titanium niobium oxide (TNO) nanoparticles were synthesized using the solvothermal method. Also, the TNO nanocomposites with three different weight ratios of MWCNTs (1, 3, and 5 wt.%) were synthesized by combining solvothermal and ultrasonication methods. The morphological analyses confirmed the formation of TNO nanoparticles with diameters of 50-70 nm and TNO/MWCNTs nanocomposites with dispersed MWCNTs through the TNO nanoparticles. Different electrochemical studies confirmed the enhancing effect of

MWCNTs on the electrochemical properties of TNO. In summary, the rate performance of TNO/MWCNTs showed an improvement of 5.6-20.11%, and also the cyclic performance showed a gain of 35-56.5%, compared with pure TNO. The electrochemical impedance spectroscopy (EIS) results showed that the charge transfer resistance and solid electrolyte interphase (SEI) resistance values were respectively decreased up to 46% and 25% by the addition of 3 wt.% MWCNTs. Furthermore, the Li-ion diffusion coefficient was increased by 28% and 148% by adding different contents of MWCNTs. In this work, TNO/3 wt.% MWCNTs showed the best electrochemical properties among all samples. The presence of MWCNTs not only facilitated the Li-ion and electron transportation by creating a fast and highly conductive network but also acted as a stress relaxing component in composite structure and held it integrated during the intercalation and deintercalation of Li-ions.

References

[1] D. Linden, Handbook of batteries, Fuel and energy abstracts, 1995, pp. 265.

[2] H. Li, Z. Wang, L. Chen, X. Huang, Research on advanced materials for Li-ion batteries, Advanced Materials, 21 (2009) 4593-4607.

[3] V. Etacheri, R. Marom, R. Elazari, G. Salitra, D. Aurbach, Challenges in the development of advanced Li-ion batteries: a review, Energy & Environmental Science, 4 (2011) 3243-3262.

[4] M. Yoshio, R.J. Brodd, A. Kozawa, Lithium-ion batteries, Springer (1) 2009.

[5] J. Jaguemont, L. Boulon, Y. Dubé, A comprehensive review of lithium-ion batteries used in hybrid and electric vehicles at cold temperatures, Applied Energy, 164 (2016) 99-114.

[6] M. Shahjalal, T. Shams, M.E. Islam, W. Alam, M. Modak, S.B. Hossain, V. Ramadesigan, M.R. Ahmed, H. Ahmed, A. Iqbal, A review of thermal management for Li-ion batteries: Prospects, challenges, and issues, Journal of Energy Storage, 39 (2021) 102518.

[7] H. Aghamohammadi, R. Eslami-Farsani, E. Castillo-Martinez, Recent trends in the development of MXenes and MXene-based composites as anode materials for Li-ion batteries, Journal of Energy Storage, (2021) 103572.

[8] H. Aghamohammadi, N. Hassanzadeh, R. Eslami-Farsani, A review study on the recent advances in developing the heteroatom-doped graphene and porous graphene as superior anode materials for Li-ion batteries, Ceramics International, 47 (2021) 22269-22301.

[9] H. Aghamohammadi, N. Hassanzadeh, R. Eslami-Farsani, A review study on titanium niobium oxide-based composite anodes for Li-ion batteries: Synthesis, structure, and performance, Ceramics International, 47 (2021) 26598-26619.

[10] Z. Zhuang, W. Wang, Y. Wei, T. Li, M. Ma, Y. Ma, Preparation of polyaniline nanorods/manganese dioxide nanoflowers core/shell nanostructure and investigation of electrochemical performances, Advanced Composites and Hybrid Materials, (2021) 1-8.

[11] X. Dong, X. Zhao, Y. Chen, C. Wang, Investigations about the influence of different carbon matrixes on the electrochemical performance of Na3V2 (PO4) 3 cathode material for sodium ion batteries, Advanced Composites and Hybrid Materials, 4 (2021) 1070-1081.

[12] C. Wang, A.J. Appleby, F.E. Little, Charge–discharge stability of graphite anodes for lithium-ion batteries, Journal of Electroanalytical Chemistry, 497 (2001) 33-46.

[13] M. Müller, L. Pfaffmann, S. Jaiser, M. Baunach, V. Trouillet, F. Scheiba, P. Scharfer, W. Schabel, W. Bauer, Investigation of binder distribution in graphite anodes for lithium-ion batteries, Journal of Power Sources, 340 (2017) 1-5.

[14] M. Lübke, I. Johnson, N.M. Makwana, D. Brett, P. Shearing, Z. Liu, J.A. Darr, High power TiO_2 and high capacity Sn-doped TiO_2 nanomaterial anodes for lithium-ion batteries, Journal of Power Sources, 294 (2015) 94-102.

[15] H. Wang, Z. Lu, L. Xi, R. Ma, C. Wang, J.A. Zapien, I. Bello, Facile and rapid synthesis of highly porous wirelike TiO_2 as anodes for lithium-ion batteries, ACS Applied Materials & Interfaces, 4 (2012) 1608-1613.

[16] M. Ko, S. Chae, J. Cho, Challenges in accommodating volume change of Si anodes for Li-ion batteries, Chemelectrochem, 2 (2015) 1645.

[17] J.M.M. de la Hoz, P.B. Balbuena, Reduction mechanisms of additives on Si anodes of Li-ion batteries, Physical Chemistry Chemical Physics, 16 (2014) 17091-17098.

[18] M. Schnabel, E. Arca, Y. Ha, C. Stetson, G. Teeter, S.-D. Han, P. Stradins, Enhanced interfacial stability of Si anodes for Li-ion batteries via surface SiO_2 coating, ACS Applied Energy Materials, 3 (2020) 8842-8849.

[19] B. Wang, B. Luo, X. Li, L. Zhi, The dimensionality of Sn anodes in Li-ion batteries, Materials Today, 15 (2012) 544-552.

[20] J. Zhang, T. Huang, Z. Liu, A. Yu, Mesoporous Fe_2O_3 nanoparticles as high performance anode materials for lithium-ion batteries, Electrochemistry Communications, 29 (2013) 17-20.

[21] H. Liu, S.-h. Luo, D.-b. Hu, X. Liu, Q. Wang, Z.-y. Wang, Y.-l. Wang, L.-j. Chang, Y.-g. Liu, T.-F. Yi, Design and synthesis of carbon-coated α-Fe_2O_3@ Fe_3O_4 heterostructured as anode materials for lithium ion batteries, Applied Surface Science, 495 (2019) 143590.

[22] X. Lv, J. Deng, B. Wang, J. Zhong, T.-K. Sham, X. Sun, X. Sun, γ-Fe_2O_3@ CNTs anode materials for lithium ion batteries investigated by electron energy loss spectroscopy, Chemistry of Materials, 29 (2017) 3499-3506.

[23] S. Goriparti, E. Miele, F. De Angelis, E. Di Fabrizio, R.P. Zaccaria, C. Capiglia, Review on recent progress of nanostructured anode materials for Li-ion batteries, Journal of Power Sources, 257 (2014) 421-443.

[24] Y. Wei, W. Luo, Z. Zhuang, B. Dai, J. Ding, T. Li, M. Ma, X. Yin, Y. Ma, Fabrication of ternary MXene/MnO_2/polyaniline nanostructure with good electrochemical performances, Advanced Composites and Hybrid Materials, 4 (2021) 1082-1091.

[25] L. Pu, J. Zhang, N.K.L. Jiresse, Y. Gao, H. Zhou, N. Naik, P. Gao, Z. Guo, N-doped MXene derived from chitosan for the highly effective electrochemical properties as supercapacitor, Advanced Composites and Hybrid Materials, (2021) 1-14.

[26] D. Xu, K. Ma, L. Chen, Y. Hu, H. Jiang, C. Li, MXene interlayer anchored Fe_3O_4 nanocrystals for ultrafast Li-ion batteries, Chemical Engineering Science, 212 (2020) 115342.

[27] Q. Li, J. Zhou, F. Li, Z. Sun, Novel MXene-based hierarchically porous composite as superior electrodes for Li-ion storage, Applied Surface Science, 530 (2020) 147214.

[28] G. Mu, D. Mu, B. Wu, C. Ma, J. Bi, L. Zhang, H. Yang, F. Wu, Microsphere-like SiO_2/MXene hybrid material enabling high performance anode for lithium ion batteries, Small, 16 (2020) 1905430.

[29] S.S. Lee, K.-T. Byun, J.P. Park, S.K. Kim, H.-Y. Kwak, I.-W. Shim, Preparation of $Li_4Ti_5O_{12}$ nanoparticles by a simple sonochemical method, Dalton Transactions, (2007) 4182-4184.

[30] J. Shu, L. Hou, R. Ma, M. Shui, L. Shao, D. Wang, Y. Ren, W. Zheng, In situ fabrication of $Li_4Ti_5O_{12}$@ CNT composites and their superior lithium storage properties, RSC Advances, 2 (2012) 10306-10309.

[31] G.-Y. Liu, H.-Y. Wang, G.-Q. Liu, Z.-Z. Yang, B. Jin, Q.-C. Jiang, Facile synthesis of nanocrystalline $Li_4Ti_5O_{12}$ by microemulsion and its application as anode material for Li-ion batteries, Journal of Power Sources, 220 (2012) 84-88.

[32] H. Yu, H. Lan, L. Yan, S. Qian, X. Cheng, H. Zhu, N. Long, M. Shui, J. Shu, $TiNb_2O_7$ hollow nanofiber anode with superior electrochemical performance in rechargeable lithium ion batteries, Nano Energy, 38 (2017) 109-117.

[33] X. Wu, J. Miao, W. Han, Y.-S. Hu, D. Chen, J.-S. Lee, J. Kim, L. Chen, Investigation on $Ti_2Nb_{10}O_{29}$ anode material for lithium-ion batteries, Electrochemistry Communications, 25 (2012) 39-42.

[34] Y. Yuan, H. Yu, X. Cheng, R. Zheng, T. Liu, N. Peng, N. Long, M. Shui, J. Shu, Preparation of $TiNb_6O_{17}$ nanospheres as high-performance anode candidates for lithium-ion storage, Chemical Engineering Journal, 374 (2019) 937-946.

[35] H. Yu, X. Cheng, H. Zhu, R. Zheng, T. Liu, J. Zhang, M. Shui, Y. Xie, J. Shu, Deep insights into kinetics and structural evolution of nitrogen-doped carbon coated $TiNb_{24}O_{62}$ nanowires as high-performance lithium container, Nano Energy, 54 (2018) 227-237.

[36] C.-A. Zhou, Z. Yao, X. Xia, X. Wang, C. Gu, J. Tu, Low-strain titanium-based oxide electrodes for electrochemical energy storage devices: design, modification, and application, Materials Today Nano, 11 (2020) 100085.

[37] L. Hu, L. Luo, L. Tang, C. Lin, R. Li, Y. Chen, Ti 2 Nb 2x O 4+ 5x anode materials for lithium-ion batteries: a comprehensive review, Journal of Materials Chemistry A, 6 (2018) 9799-9815.

[38] H. Kim, Y. Lee, D. Byun, W. Choi, $TiNb_2O_7$ microsphere anchored by polydopamine-modified graphene oxide as a superior anode material in lithium-ion batteries, International Journal of Energy Research, 44 (2020) 4986-4996.

[39] A. Ashish, P. Arunkumar, B. Babu, P. Manikandan, S. Sarang, M. Shaijumon, $TiNb_2O_7$/Graphene hybrid material as high performance anode for lithium-ion batteries, Electrochimica Acta, 176 (2015) 285-292.

[40] S. Jayaraman, V. Aravindan, P. Suresh Kumar, W. Chui Ling, S. Ramakrishna, S. Madhavi, Exceptional performance of $TiNb_2O_7$ anode in all one-dimensional architecture by electrospinning, ACS Applied Materials & Interfaces, 6 (2014) 8660-8666.

[41] S. Lou, X. Cheng, Y. Zhao, A. Lushington, J. Gao, Q. Li, P. Zuo, B. Wang, Y. Gao, Y. Ma, Superior performance of ordered macroporous $TiNb_2O_7$ anodes for lithium ion batteries: understanding from the structural and pseudocapacitive insights on achieving high rate capability, Nano Energy, 34 (2017) 15-25.

[42] H. Song, Y.-T. Kim, A Mo-doped $TiNb_2O_7$ anode for lithium-ion batteries with high rate capability due to charge redistribution, Chemical Communications, 51 (2015) 9849-9852.

[43] S. Deng, H. Zhu, B. Liu, L. Yang, X. Wang, S. Shen, Y. Zhang, J. Wang, C. Ai, Y. Ren, Synergy of Ion Doping and Spiral Array Architecture on $Ti_2Nb_{10}O_{29}$: A New Way to Achieve High-Power Electrodes, Advanced Functional Materials, 30 (2020) 2002665.

[44] C. Lin, L. Hu, C. Cheng, K. Sun, X. Guo, Q. Shao, J. Li, N. Wang, Z. Guo, Nano-$TiNb_2O_7$/carbon nanotubes composite anode for enhanced lithium-ion storage, Electrochimica Acta, 260 (2018) 65-72.

[45] M. Liu, H. Dong, S. Zhang, X. Chen, Y. Sun, S. Gao, J. Xu, X. Wu, A. Yuan, W. Lu, Three-dimensional porous $TiNb_2O_7$/CNT-KB composite microspheres as lithium-ion battery anode material, Chemelectrochem, 6 (2019) 3959-3965.

[46] G. Zhu, W. Jiao, Q. Li, Y. Zhao, X. Liu, R. Che, Conductivity optimization via intertwined CNTs between $TiNb_2O_7$@ C microspheres for a superior performance Li-ion battery anode, Journal of Colloid and Interface Science, 607 (2022) 1103-1108.

[47] Y. Yang, Y. Li, K. Liu, K. Zhang, S. Jin, Y. Bao, Y. Fan, Z. Yang, R. Zhang, B. Jin, Hierarchical porous $TiNb_2O_7$@ N-doped carbon microspheres as superior anode materials for lithium ion storage, International Journal of Hydrogen Energy, 46 (2021) 3425-3436.

[48] Y. Yang, Y. Yue, L. Wang, X. Cheng, Y. Hu, Z.-z. Yang, R. Zhang, B. Jin, R. Sun, Facile synthesis of mesoporous $TiNb_2O_7$/C microspheres as long-life and high-power anodes for lithium-ion batteries, International Journal of Hydrogen Energy, 45 (2020) 12583-12592.

[49] B.-G. Lee, S.-H. Lee, H.-J. Ahn, J.-R. Yoon, High performance hybrid supercapacitors using granule $Li_4Ti_5O_{12}$/Carbon nanotube anode, Journal of Alloys and Compounds, 748 (2018) 882-888.

[50] S. Zhao, M. Zhang, Z. Wang, X. Xian, Enhanced high-rate performance of $Li_4Ti_5O_{12}$ microspheres/multiwalled carbon nanotubes composites prepared by electrostatic self-assembly, Electrochimica Acta, 276 (2018) 73-80.

[51] S. Zhao, O. Ka, X. Xian, L. Sun, J. Wang, Effect of primary crystallite size on the high-rate performance of $Li_4Ti_5O_{12}$ microspheres, Electrochimica Acta, 206 (2016) 17-25.